Atomic collisions in the presence of intense, ultrashort laser pulses

T. Sizer II* and M. G. Raymer
The Institute of Optics, University of Rochester, Rochester, New York 14627
(Received 19 February 1987)

The interaction of ultrashort laser pulses and colliding atoms has been studied theoretically and experimentally. Solutions to the semiclassical Schrödinger equation in Bloch-equation form predict the effect of pulses whose duration is shorter than the collision duration. These results have been applied to the process $Na(3S) + Ar + \hbar\omega \rightarrow Na(3P_{1/2}) + Ar$ using intense, off-resonant laser pulses with variable temporal duration. It has been found that at a fixed laser intensity the efficiency of exciting the $Na(3P_{1/2})$ state is higher for ultrashort pulses than for pulses with duration longer than the collision duration. This effect is caused by a time-dependent modification of the collision potentials by the intense laser field. The theoretical calculation is in qualitative agreement with the experimental results, although a large discrepancy exists between the predicted and observed laser power needed to observe the increased efficiency with short pulses.

I. INTRODUCTION

Atomic collisions in the presence of light emission and absorption have long been studied both theoretically and experimentally. Before the advent of the laser, many of the basic processes involving colliding atoms had been studied. As lasers were used in the studies, however, it became apparent that the laser could be used not only as a tool to investigate the collision process, but also to manipulate or control the process. A large number of theoretical predictions have been reported[1–7] describing the possibility that an intense field could modify the collision dynamics, and thus change its outcome, but only a few experiments published to date have shown evidence for such effects.[8–12] The term "modified collision dynamics" means here that the potential energy surfaces which govern the collision dynamics are distorted by the ac Stark effect induced by the intense laser field. This results in altered probabilities for the scatterers to end up in certain outgoing channels. The attractiveness of the idea of modified collisions, of course, lies in the possibility of selectivity controlling physical or chemical processes by judicious choice of laser frequency and intensity.

Lisitsa and Yakovlenko[1] first described nonlinear optical effects in atomic collisions more than ten years ago. They described the intensity dependence of what they called an optical collision—the absorption of a photon with frequency in the collision-broadened line wing of an allowed transition. This process has also been termed collisional redistribution[13,14] and laser-induced collisional energy transfer.[6] Lisitsa and Yakovlenko predicted that for laser pulses with duration longer than the collision duration the cross section for the optical collision should decrease at high intensities.

Carlsten, Szöke, and Raymer[14] made the first studies of the dependence of the collisionally redistributed signal on the laser detuning, laser intensity, and buffer gas pressure. The pulses used for these experiments were much longer than both the collision duration and the time between collisions, so the results were due to multiple collisions rather than to individual collisions. For this reason, together with the experimental effects of spatial averaging and radiation trapping, the decrease in optical-collision cross section at high laser intensities was difficult to observe.[15]

Light and Szöke[4] pointed out that the ideal two-state model for the target atom, used by previous researchers because of its simplicity, did not adequately describe the optical collision dynamics correctly since the different collisional potentials associated with the excited level can all interact with the laser field. Kleiber *et al.*[10] observed this spatial degeneracy effect in the Sr-Ar collision system by using an intense 7-nsec pulse to excite the $m_j = 0, +1, -1$ resonance levels at 460 nm in the Sr atom. Agreement was found between the theoretical predictions[7] and the experimental results of Kleiber *et al.*[10] when observing the depolarization of the collision-induced resonance fluorescence as a function of the laser intensity.[16] These results indicate that the influence of multiple excited states should be taken into account when interpreting experimental results.

The present paper is an expanded discussion of our recently reported experimental and theoretical study[17] of collisional redistribution of light using laser pulses that are shorter than the duration of a collision (1–3 psec). It was first proposed by Lee and George[5] that choosing the duration of the laser pulse to be this short allows the experimenter to change actively the shape of the potentials during the collision. In principle, if one can open and close reactive channels at appropriate times during the collision, one can strongly influence its outcome. The intent of this work is to study the modification of atomic-collision dynamics due to an intense laser pulse whose duration is shorter than the collision itself.

When two atoms collide their proximity causes a time-dependent shifting of their combined energy levels. A schematic representation of the potential energy variation with respect to the interatomic separation R is shown in Fig. 1. If one applies a laser pulse to the col-

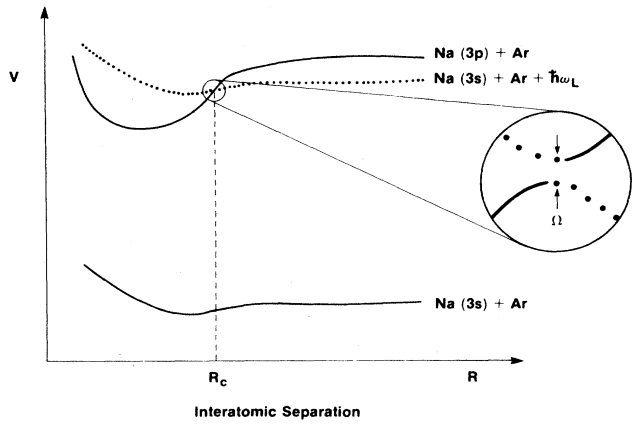

FIG. 1. Simplified schematic of potential energy curves for the collision system Na+Ar. The laser-induced dressed state is shown as a dotted line. The avoided crossing region is enlarged for clarity.

lision system one creates a dressed state which is a copy of the ground state raised in energy by the energy of one laser photon $\hbar\omega_L$. Through judicious choice of ω_L, the dressed state, shown as the dotted line in Fig. 1, and the excited state can be made to intersect at a particular interatomic separation R_c. Given that the distance of closest approach (impact parameter) for the atomic collision is less than R_c, there are two points in space and time where curve crossings occur. This is illustrated in Fig. 2 for a straight-line trajectory. When the atoms are at separation R_c the laser is "in resonance" with the excited state and population can, near this point, be moved from the ground to the excited state. If one of the atoms ends up in its excited state, it is said that an optical collision,[1,9] or collisional redistribution,[4,7,10,13,14] has taken place. The time between the resonances or curve crossings, T_c, can be calculated for a straight-line trajectory knowing the radius R_c, the impact parameter b, and the relative velocity of the colliding atoms. This time will be

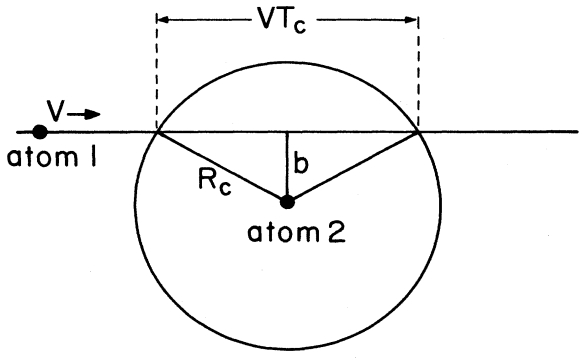

FIG. 2. Geometry of the colliding atoms. In this reference frame the perturbing atom moves by the target atom with a velocity V and an impact parameter b. Avoided crossings occur at separation R_c.

used to define "long" laser pulses as those whose duration is greater than T_c, and "short" pulses as those temporal duration is shorter than T_c. A long laser pulse therefore can interact with both curve crossings whereas a short pulse can interact with only one.

When two states cross, either two real states or a real state and a dressed state, they avoid one another if there is an interaction between them. In the present case this interaction is due to the ac Stark effect, with the smallest separation between the two levels being given by the Rabi frequency, $\Omega = d_{12}E/\hbar$, where d_{12} is the dipole matrix element between the ground and excited states and E is the laser electric field amplitude. This avoided crossing is shown in Fig. 1 for the case of Na+Ar collisions. The probability p of jumping across the avoided crossing during a single pass through the crossing region decreases as the laser field E increases, since the motion on the potentials becomes more adiabatic.

The probability of moving from the dressed ground state to the excited state in the course of a completed collision is different for the cases of long and short pulses. In the long pulse case, where the avoided crossing is encountered twice, this probability is given by the probability of not jumping across the avoided crossing on the first pass but jumping on the second, plus the probability of jumping on the first pass but not on the second, or

$$P_{\text{long}} = 2p(1-p) . \tag{1}$$

In contrast, the short pulse case is illustrated in Fig. 3. At times before the laser pulse is present the target atom is in the ground state and is colliding with a perturber atom. When the laser pulse is turned on the target atom is placed in the dressed state and passes through the avoided-crossing region. When passing through this region, however, if the target atom does not "jump" across the avoided crossing then it adiabatically moves onto the excited-state potential. The dressed state then disappears, due to the laser pulse turning off, before the atoms can pass through a curve crossing again. When this happens the target atom is trapped on the excited-state potential curve. Thus the probability of ending up in the excited state in this case is

$$P_{\text{short}} = 1-p \tag{2}$$

or the probability of *not* jumping across the avoided crossing. One can see that at high laser intensites (small values of p) there is potentially great advantage in using short pulses ($P_{\text{short}} \to 1$) rather than long pulses ($P_{\text{long}} \to 0$).

In 1980 Bonch-Bruevich *et al.*[9] made the first experimental observations of the decrease in optical cross section at high laser intensities as predicted in Eq. (1). For this they used a frequency-doubled Nd:glass laser with pulse duration of 10 psec at a wavelength of 530 nm, which happens to be 50 Å detuned to the red side of a Tl resonance line. This value of the pulse duration is greater than T_c so it is considered long, however, it is shorter than the time between collisions. Although the predicted nonlinearity did occur, it required a much higher laser intensity (10^9 W/cm^2) than theoretically

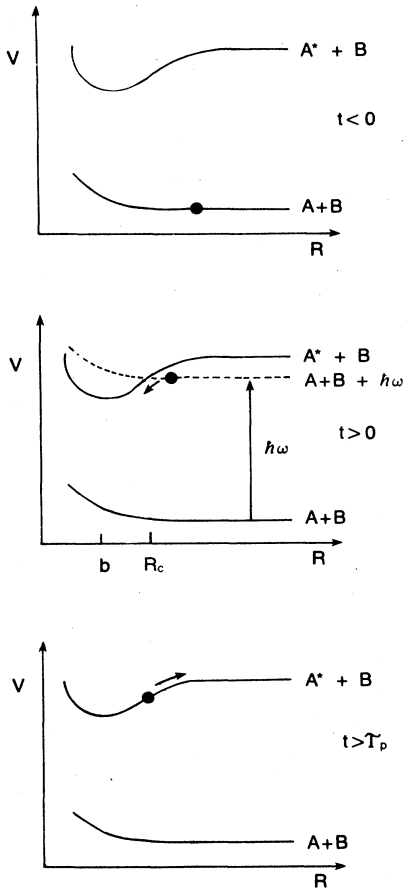

FIG. 3. Potential energy vs internuclear separation for three different points in time illustrating how a short pulse can be used to provide excited-state population through purely adiabatic motions.

predicted (10^6 W/cm^2).

This paper will outline our studies of the pulse-duration dependence of modified atomic-collision dynamics. First the simple Landau-Zener model is described. In order to treat more completely the theoretical aspects of this interaction, a fairly rigorous semiclassical theory using optical Bloch equations is presented which describes the collisional interaction when a realistically shaped pulse whose duration is shorter than a collision duration is applied. The theory is described in Sec. II. Section III presents the results of an experimental study that yields evidence for the pulse-duration dependence. For the experiments an intense, stable, high-repetition-rate source of tunable ultrashort pulses was developed.

II. THEORETICAL STUDY

In this section we present a discussion of the Landau-Zener model, and also discuss in detail the numerical solutions of the Schrödinger equation describing the collision.

It should be pointed out here that the laser is assumed to be detuned far from the resonance line of the absorbing atom, which results in the collision being in the quasistatic, or quasimolecular, regime. This occurs when the laser detuning is much greater than the inverse of the collision duration, which is approximated by T_c, the time between curve crossings. This time is typically several picoseconds, corresponding to a detuning of several wave numbers. For detunings much less than several wave numbers, the collisions take place in the impact regime. The line broadening in this regime results from many impulselike collisions.

For laser detunings much greater than several wave numbers, as in the present case, the line broadening is in the quasistatic regime, and can be viewed as resulting from photon absorption between the potentials of a single collisional event. This viewpoint has led to successful efforts to determine collision potentials by measuring far-wing absorption or emission profiles.[18,19]

For the present case of Na-Ar collisions we take the diabatic (noncrossing) potentials to be described in the region of interest by a simple Van der Waals interaction. The difference between the excited-state potential V_2 and the ground-state potential V_1 is thus given by

$$V_2(R)-V_1(R)=\hbar(\omega_0-C_6/R^6)\ , \tag{3}$$

where ω_0 is the atomic sodium resonance frequency and C_6 is equal to 3.8×10^{-31} cm^6 rad/sec.[19] Also, note that for the NaD_1 line, $d_{12}=1.1\times10^{-17}$ esu cm.[20]

A. Landau-Zener model

Landau,[21] Zener,[22] and Stueckelberg[23] independently derived forms of the "Landau-Zener formula," which describes the probability of jumping across the avoided crossing on a single pass. (See Fig. 1). The following assumptions were made. First, the energy difference across the avoided crossing is much less than the kinetic energy of the colliding pair so that the loss in kinetic energy is negligible during a jump across the avoided crossing. Second, the transition region is so small that within it the detuning between the diabatic potentials is approximately a linear function of interatomic separation and thus of time. Third, only two collision potentials are involved in the dynamics. Given these assumptions and by using the Weber function they obtained the probability p of jumping across the avoided crossing as

$$p=e^{-W}\ , \tag{4}$$

where

$$W=\frac{2\pi\hbar\Omega^2}{V\left|\dfrac{\partial V_2}{\partial R}-\dfrac{\partial V_1}{\partial R}\right|_{R_c}}\ , \tag{5}$$

V is the internuclear velocity, and $\hbar\Omega$ is the off-diagonal Hamiltonian matrix element, a measure of the interaction strength. In the case of optical collisions Ω is the Rabi frequency, which is proportional to laser field strength. Thus the collisional interaction is controllable by the experimenter.

As described in the Introduction, the probability of ending up in the excited state after a collision in the presence of a long laser pulse, which allows two curve crossings , is $2p(1-p)$, or

$$P_{\text{long}}=2e^{-W}(1-e^{-W}) . \tag{6}$$

This probability is plotted in Fig. 4. The intensity at which the maximum excitation probability occurs is denoted I_{crit}. It is related to the critical field E_{crit} by the relation

$$I_{\text{crit}}=\frac{c}{8\pi}E_{\text{crit}}^2 , \tag{7}$$

where I_{crit} is in units of ergs/sec cm^2, E_{crit} is in units of statvolts/cm and c is in units of cm/sec. From Eqs. (5)–(7), I_{crit} is found to be

$$I_{\text{crit}}=0.69\hbar c V\left|\frac{\partial V_2}{\partial R}-\frac{\partial V_1}{\partial R}\right|_{R_c} . \tag{8}$$

The values for I_{crit} and E_{crit} will be used throughout this work to indicate the point at which the nonlinearity in the excitation probability occurs.

Equation (8) can be used to estimate I_{crit} for the Na-Ar collision illustrated in Fig. 1 and studied experimentally. Using the values C_6 and d_{12} quoted earlier, and $V=5\times10^4$ cm/sec for a typical thermal velocity, yields $I_{\text{crit}}=7.4\times10^6$ W/cm^2.

In the case of a laser pulse shorter than the collision duration, as described in the Introduction, the probability of ending up in the excited state after the collision is $(1-p)$, or

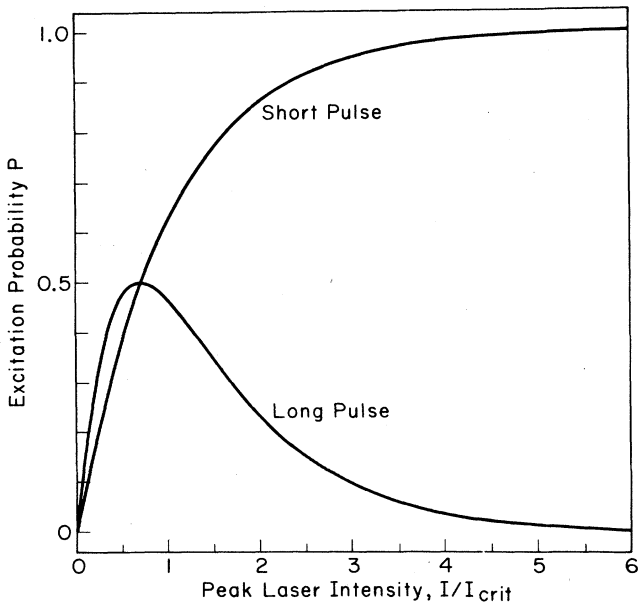

FIG. 4. Landau-Zener absorption probabilities for laser-pulse durations which are long or short compared to the time T_c between avoided crossings.

$$P_{\text{short}}=1-e^{-W} , \tag{9}$$

which is also plotted in Fig. 4. At high laser intensity the probability goes to unity, in contrast to the result for the long pulse. This was first pointed out by Lee and George,[5] using a somewhat extended version of the Landau-Zener formula. The main limitations of their approach are in using temporally square laser pulses and assuming the validity of the Landau-Zener model.

The Landau-Zener model, although useful due to its simplicity, has a number of well-known deficiencies. The first is the assumption that the transitions can occur only in a small region very near the curve crossing point.[24] This is in fact not the case. The transition region is a vaguely defined zone around the curve crossing which is defined by not only the interaction strength but also the slopes of the two intersecting potential curves. Although it is most probable that transitions will be made at the point at which the two adiabatic potentials are the closest, there is a finite probability that transitions can be made nearby. At high field strengths where the potentials are well separated, the transition region can become quite large and the assumption that the two potentials can be approximated by straight lines over the region becomes invalid. The second error results from adding the probabilities at the two crossings incoherently. This neglects the quantum-mechanical (Stueckelberg) oscillations of excitation probability that occur as a function of, for example, velocity. Often these oscillations average out in an experimental situation.

B. Bloch-equation theory of picosecond optical collisions

1. Model and equations of motion

In order to describe more accurately the collision dynamics in the presence of picosecond optical pulses, a theory has been developed that involves the solution of the two-level semiclassical Schrödinger equation in Bloch-equation form. Several of the difficulties with the Landau-Zener result used by Lee and George have been avoided in taking this approach.

Several assumptions and approximations were made in developing this theory which ought to be detailed. They are as follows.

(i) Straight-line classical trajectories are assumed with no change in the atomic velocities over the course of the collision.

(ii) The input laser pulse shape is Gaussian with variable pulse duration.

(iii) The difference potential (V_2-V_1) has a R^{-6} shape in the case of van der Waals collisions.

(iv) The transition dipole moment d_{12} corresponds to an allowed transition and is independent of R.

(v) The time between collisions is much longer than the collision duration and the laser pulse duration so that the effects of multiple collisions are ignored.

(vi) The laser pulse duration is much shorter than the radiative lifetime, so that radiative damping is ignored.

(vii) The impact parameter for each collision is determined by thermally random motions of the atoms.

(viii) The time of closest approach can occur at any

time with respect to the maximum of the laser pulse. This time is averaged over.

(ix) No coupling terms are included to account for the effects of nuclear motions or the translational motion of the electron when it is excited from an S to P state.[23]

(x) The laser frequency is near a resonance of one of the colliding atoms and the rotating-wave approximation is valid.

(xi) There is only one excited state and one ground state, providing a pure two-state system with assumed spherically symmetric potentials.

(xii) It is assumed to be sufficient to calculate the dynamics at a single velocity, rather than averaging over the Maxwell-Boltzmann velocity distribution.

Light and Szöke[4] have illustrated the need to treat the system as more than a two-state system. They showed that in the case of Sr-Ar collisions, for which the excited Sr(P) level has three-fold spatial degeneracy, the rapid decrease of excitation probability with increasing laser intensity (for a long pulse) is dramatically slowed down when the degeneracy is taken into account. This occurs because the coupling of the z-polarized laser field to the (asymptotic) $m_j=\pm 1$ states is weaker than the coupling to the $m_j=0$ state. Therefore, the $m_j=\pm 1$ states require much higher field strengths for adiabatic dynamics to dominate. This effect also leads to a strong depolarization of the emitted fluorescence.[10] We were not able to take spatial degeneracy into account due to the already lengthy nature of the present numerical calculations. This occurs in part because of the need to average over the time of closest approach, which is not necessary in the usual case of steady laser intensity.

The two-level Schrödinger equation written in Bloch-equation form is given as[25]

$$\dot{u}=-[\omega_0(t)-\omega_L]v \ , \tag{10a}$$

$$\dot{v}=[\omega_0(t)-\omega_L]u+\kappa E(t)w \ , \tag{10b}$$

$$\dot{w}=-\kappa E(t)v \ , \tag{10c}$$

where u and v are the in-phase and in-quadrature components of the atomic dipole moment, w is the single-atom population difference or inversion, ω_L is the laser frequency, $E(t)$ is the magnitude of the laser electric field, and κ is a measure of the strength of the atomic line, defined by

$$\kappa\equiv\frac{2d_{12}}{\hbar} \ , \tag{11}$$

where d_{12} is the magnitude of the atomic dipole-matrix element. The time dependence of the resonance frequency $\omega_0(t)$ comes about due to the shifting of the energy levels as the atoms collide.

The form of $\omega_0(t)$ can be determined knowing the type of collision (resonance or van der Waals) together with the assumption of straight-line atomic trajectories. The interatomic separation as a function of time is

$$R(t)=\left[(b^2+V^2(t-t_0^2)\right]^{1/2} \ , \tag{12}$$

where b is the impact parameter, V is the relative velocity, and t_0 is the time of closest approach between the two colliding atoms. In the case of van der Waals collisions the resonance frequency as a function of time is thus

$$\omega_0(t)=\omega_0-\frac{C_6}{[b^2+V^2(t-t_0)^2]^3} \ . \tag{13}$$

When using laser pulses of the order of 1 psec in duration there is a sizeable spectral bandwidth associated with it due to the uncertainty principle. This large bandwidth does not have to be taken explicitly into account in the equations; its effect is seen by solving Eq. (10) for the temporal dynamics.

The Bloch equations have a conservation relation which can be used to advantage. The values u, v, and w are related (since we can ignore relaxation when using picosecond pulses) through the equation[25]

$$u^2+v^2+w^2=1 \ . \tag{14}$$

Testing whether this relation was satisfied provided an easy method to check on the accuracy of the numerical solution.

An example of the numerical solution of Eq. (10) is displayed graphically in Fig. 5 for the case of Na-Ar ex-

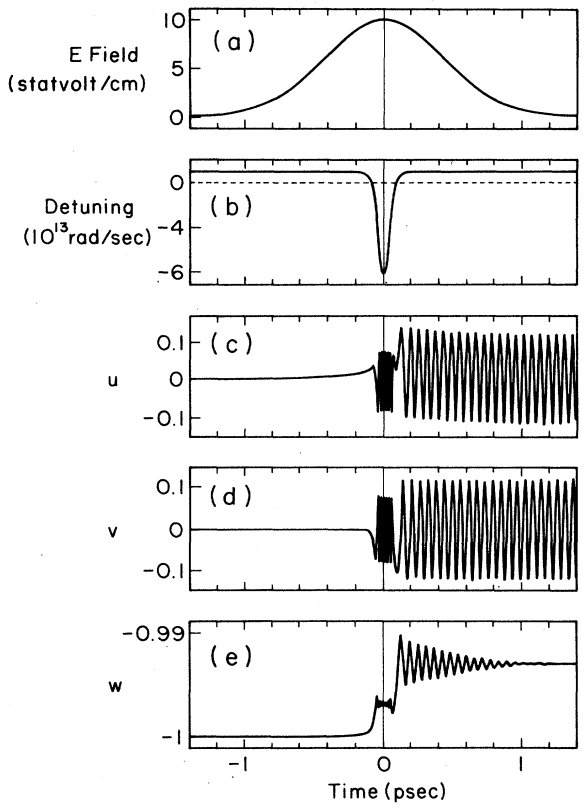

FIG. 5. Differential-equation solutions for single Na-Ar collision event. In this figure (a) is the applied electric field strength, (b) is the detuning variation due to the collision, (c) and (d) are in-phase (u) and in-quadrature (v) components of the atomic dipole, and (e) is the population inversion (w) and is related to the excited-state probability by $(w+1)/2$.

cited by a 10-psec pulse. The relative velocity is 5×10^4 cm/sec. The laser field amplitude, whose peak value is 25 statvolt/cm is shown in 5(a). The detuning $[\omega_0(t)-\omega_L]$, plotted in Fig. 5(b) illustrates that a 10-psec pulse is a long pulse since the two points in time at which the detuning goes through zero (system passes through a curve crossing) are separated by a time less than 10 psec. The active atom starts in the ground state ($w=-1$). The end result of w plotted in Fig. 5(e) is, of course, the quantity of interest since it represents the probability for an atom to be excited during the optical collision. One notices that there is change in this value only during the zero crossings in the detuning, as expected.

Several modifications were made in the numerical method to decrease the computing time required for solution. First, note that the instantaneous frequency of oscillation (generalized Rabi frequency) Ω' of the Bloch pseudospin vector (u,v,w) is given by[25]

$$\Omega'(t)=\{\kappa^2E^2(t)+[\omega_0(t)-\omega_L]^2\}^{1/2}\ . \tag{15}$$

One observes that at high laser electric field strengths or large detunings the oscillation frequency increases, making numerical accuracy difficult to maintain. Therefore, the temporal step size was made inversely related to the generalized Rabi frequency, providing an error less than 10^{-3} in each differential equation. Second, since there is virtually no change in the vlaue of w before the first curve crossing, even in the presence of the electric field, the numerical solution was started just before the first crossing. The pseudospin vector (u,v,w) was initialized by assuming that it adiabatically follows the movement of the effective field vector, $(\Omega,0,\omega_0(t)-\omega_L)$ prior to the curve crossing. The initial values for u v, and w at $t=t_i$ are thus[25]

$$u(t_i)=\frac{\kappa E(t_i)}{\{\kappa^2E^2(t_i)+[\omega_0(t_i)-\omega_L]^2\}^{1/2}}\ , \tag{16a}$$

$$v(t_i)=0\ , \tag{16b}$$

$$w(t_i)=\frac{-[\omega_0(t_i)-\omega_L]}{\{\kappa^2E^2(t_i)+[\omega_0(t_i)-\omega_L]^2\}^{1/2}}\ . \tag{16c}$$

And third, after the second curve crossing the pseudospin vector is precessing around the effective field vector and will continue to do so until the dipole decays spontaneously. While the laser pulse is still present, however, there are decreasing Rabi oscillations present on the inversion w which impede obtaining its final value. The angle between the effective field vector and pseudospin vector stays constant over the remainder of the laser pulse in an adiabatic following form similar to that assumed prior to the first curve crossing. Therefore, the final value can be calculated knowing the instantaneous value of u, v, and w at t_f, just after the second curve crossing. The final value for w as a function of the instantaneous values of u, v, and w, and E at a time $t=t_j$ is thus calculated to be

$$w(\text{final})=\frac{-\kappa E(t_f)u(t_f)+[\omega_0(t_f)-\omega_L]w(t_f)}{\{\kappa^2E^2(t_f)+[\omega_0(t_f)-\omega_L]^2\}^{1/2}}\ . \tag{17}$$

These three modifications combined to reduce the computation time by a factor of 30.

The final excited-state population has been calculated for different peak electric field strengths for both long and short pulses, as shown in Fig. 6. The long pulse has a duration [full width at half maximum (FWHM) of intensity] of 10 psec, and is maximum at the time of closest approach. The short pulse duration is 1.6 psec, and is maximum at the first curve crossing. The long-pulse curve rises and falls in a fashion similar to that observed in both the Landau-Zener model and the Lee and George model. The value $E_{\text{crit}}=220$ statvolt/cm at which the probability is maximum corresponds to a laser intensity of $I_{\text{crit}}=5.8$ MW/cm^2, as compared to 7.4 MW/cm^2 predicted by the simple Landau-Zener formula [see Eq. (8)]. The main result is that in the short-pulse case the population does not decrease at high field strength, in qualitative agreement with Fig. 4.

2. *Nonadiabatic excitation of noncolliding atoms*

Whenever one applies a pulsed laser field detuned somewhat from a resonance line there is a finite probability that direct excitation of the line can occur without the aid of a collision, thereby complicating interpretation of the results. The effect of this competing process was modeled using the same numerical solution as before but with the time-dependent detuning replaced by the static atomic detuning. The results for a 1.6-psec pulse are plotted in Fig. 7. A 10-psec case was also run, however, there was virtually zero contribution to the population over the entire range of electric field strengths. In Fig. 7 the excited-state population can be seen to increase with increasing electric field strength. Of course, the pseudospin vector does not adiabatically follow the effective field

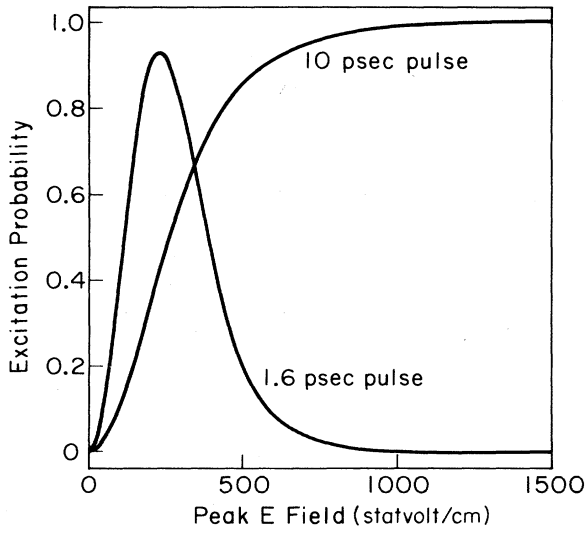

FIG. 6. Final values of excitation probability $(w+1)/2$ vs peak applied electric fields for short and long laser pulses. The laser detuning is 15 Å (43 cm^{-1}), and $V=5\times10^4$ cm/sec, $b=2$ Å.

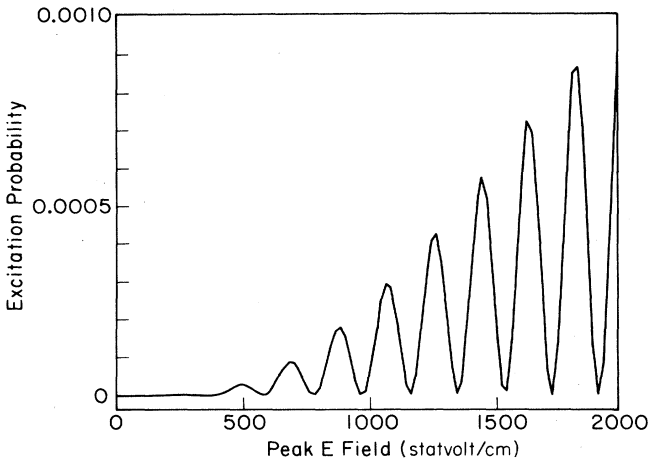

FIG. 7. Nonadiabatic excitation probability of noncolliding atoms when a 1.6-psec pulse is applied. Parameters same as in Fig. 6.

exactly, and the following gets less accurate as one increases the rate of change of electric field strength, either by increasing the peak electric field or by decreasing the pulse duration. Nevertheless, even at ten times the value of E_{crit} for the case of a 1.6-psec pulse the probability of excitation in the absence of a collision is less the 1%.

Since all atoms, not just those undergoing collisions, will be nonadiabatically excited with probability on the order of 1%, this could form a significant background signal in comparison with the signal arising from atoms undergoing collisions during the laser pulse. The fraction of such atoms is estimated by $N_P 2\pi R_c^2 V \tau_p$, where N_P is the perturber density and τ_p is the pulse duration. For a 1.6-psec pulse a typical experimental situation (see later) yields a fraction of 0.4%, comparable to the nonadiabatic excitation fraction. This effect will be discussed further in the experimental part of the paper.

3. *Variation in probability with respect to b and t_0*

Since the experiments are to be done in a vapor cell where there is no control over either the time of closest approach between colliding atoms (t_0) or the impact parameter of the collisions (b), one must average the results over all the possible values of these two variables. In order to find the range that must be integrated over, numerical solutions were made with different values of both b and t_0, with the laser pulse having its maximum at $t=0$.

The variation in excitation with changing impact parameter is graphed in Fig. 8. Figure 8(a) is the dependence for a short 1.6-psec pump pulse whereas Fig. 8(b) is the dependence for a long 10-psec pulse. For both examples the peak of the laser pulse was timed to be at the point of closest approach of the colliding atoms (i.e., $t_0=0$). In the long-pulse case the peak field strength is below the value of E_{crit} and there is a great deal of oscillation due to the coherence between the two curve crossings. Obviously there is still a large excitation probability even at the small impact parameters, which must be taken into account. The short-pulse case shows less oscillation since only one of the two curve crossings can be addressed strongly. With the laser pulse temporally centered on the time of closest approach of the atoms, curve crossings occur only when the atomic trajectory is approximately tangent to the circle of radius R_c (i.e., $b \simeq R_c = 6.0$ Å). The excitation probability extends all the way to 6.75 Å before it goes to zero, indicating that we can indeed obtain excited-state population without the benefit of a curve crossing as predicted by Bates.[24] These curves indicate that one must take into account impact parameters out to about 7 Å when averaging over impact parameter.

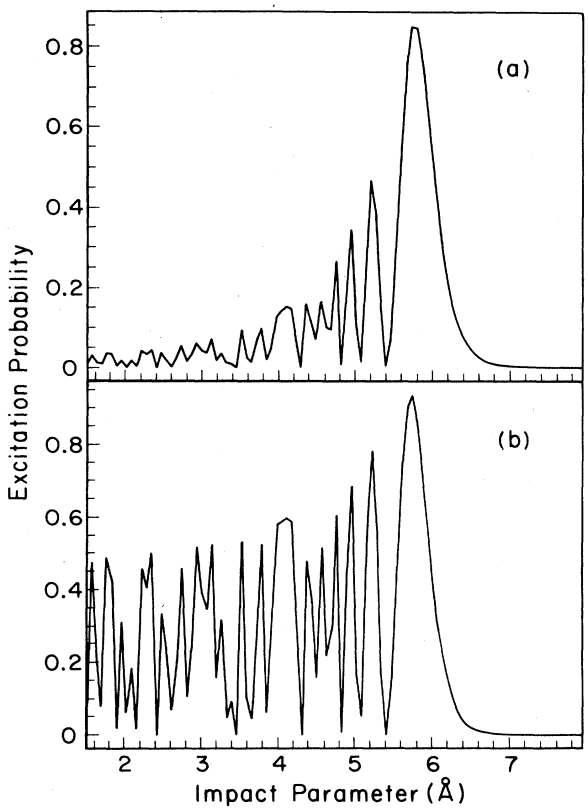

FIG. 8. Variation of excitation probability with impact parameter. In case (a) a 1.6-psec pulse was used while in (b) a 10-psec pulse was used. In both cases the E field is 100 statvolt/cm (less than E_{crit}), the peak of the pulse is centered in time over the time of closest approach, and the laser detuning is 15 Å.

The dependence of excitation probability on t_0, the difference in time between the peak of the laser pulse, and the point of closest approach between the two atoms is plotted in Fig. 9. In this case R_c was again 6.0 Å, the impact parameter was 2 Å, and the peak applied E field was 100 statvolt/cm. With a velocity of 5×10^4 cm/s, it takes 2.3 psec to move from one curve crossing to the other. In the 1.6-psec-pulse case the two curve-crossing points are well resolved from each other, while in the

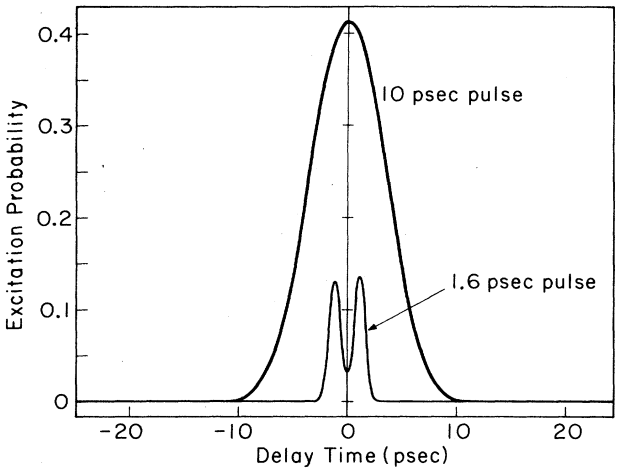

FIG. 9. Variation of excitation probability with time delay between the time of closest approach and the peak of the laser pulse. The peak E field was 100 statvolt/cm (less than E_{crit}), the impact parameter was 2 Å, the laser detuning was 15 Å, and $V=5\times10^4$ cm/s.

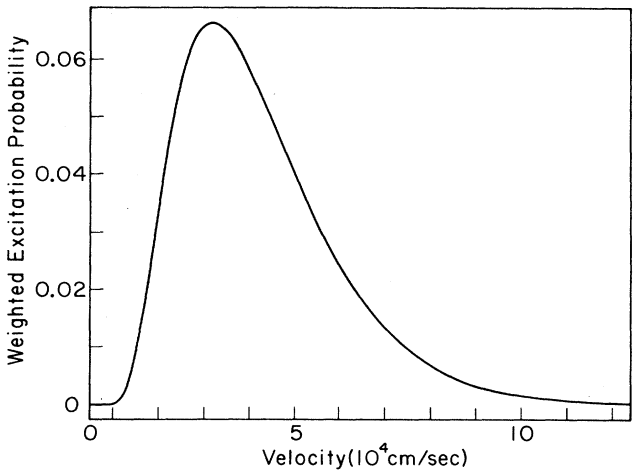

FIG. 10. Variation of weighted excitation probability with interatomic velocity. In this case a 1.6-psec pulse was used at an E field of 50 statvolt/cm (less than E_{crit}), the impact parameter was 2 Å, and the laser pulse was centered in time over the first curve crossing. The probability has been weighted by a Maxwell-Boltzmann velocity distribution with a mean velocity of 5×10^4 cm/sec.

10-psec-pulse case the two curve crossings are indistinguishable since the laser pulse overlaps both of them. These two curves indicate that one must average over a time which is the greater of four times the pulse duration (FWHM) of the laser pulse or the time that it takes the atoms to move apart sufficiently that the detuning is large enough that there is no chance of excitation. From these two curves it is found that this occurs at an interatomic separation of 9.4 Å for the case of Na-Ar collisions.

4. *Variation in probability with respect to velocity*

The velocity dependence of the picosecond optical collision dynamics was tested by varying the velocity used in the numerical solutions. The final excitation probability, weighted by the Maxwell-Boltzmann velocity distribution, is plotted in Fig. 10 for a 1.6-psec input pulse with a peak electric field strength of 50 statvolt/cm, occurring at the first curve crossing. Equations (5) and (9) from the Landau-Zener model indicates that lower velocities would lead to a higher excitation probability than would higher velocities. This is indeed the case. However, when the probability is weighted by the Maxwell-Boltzmann velocity distribution the peak occurs near the mean velocity (5×10^4 cm/sec.)

Although there is obviously a dependence on the velocity in the numerical solution, it was not averaged over to obtain the final results. The averaging with respect to one of the three experimental variables (impact parameter, time of closest approach, and velocity) had to be eliminated due to computer time limitations, and the velocity dependence was not as strong as the other two.

5. *Average over b and t_0*

In order to average over the possible value of b and t_0, probabilities must be calculated for different values of b and t_0 to occur. The details of this calculation are given in the Appendix. If we denote by $P_{\text{ex}}(E,\tau_p,\Delta_L,b,t_0)$ the probability of excitation by a laser pulse with peak field strength E occurring at $t=0$, duration τ_p, and detuning Δ_L, given an impact parameter b and time of closest approach t_0, then the number of atoms excited per unit volume is given by

$$N_{\text{ex}}(E,\tau_p,\Delta_L) = N_P N_A^2 2\pi V \int_0^B \int_{-T_0}^{T_0} P_{\text{ex}}(E,\tau_p,\Delta_L,b,t_0) b\, db\, dt_0 , \tag{18}$$

where N_P and N_A are the perturber and target atom densities and V is the velocity. B and T_0 are the practical integration limits of b and t_0, outside of which P_{ex} is negligible.

Note that if P_{ex} is independent of t_0 and if E is constant, then

$$N_{\text{ex}}(E,\Delta_L)=N_P N_A \sigma V 2T_0 , \tag{19}$$

where the collision cross section is given by

$$\sigma=2\pi \int_0^B P_{\text{ex}}(E,\Delta_L,b) b\, db , \tag{20}$$

which is the usual expression. In the present case, however, a time-independent cross section cannot, strictly speaking, be defined. It may still be useful, nevertheless, to define a quasi-cross-section by

$$\sigma=\frac{N_{\text{ex}}(E,\tau_p,\Delta_L)}{N_P N_A V \tau_p} . \tag{21}$$

Preliminary runs were made to decide how many different values of b and t_0 were needed to integrate ade-

quately over their respective ranges. It was found that 50 values were needed to average over b and 20 values were needed to average over t_0. Although even 50 values of b do not follow exactly the fast oscillation evident in Fig. 8, the large number of values used and the varying oscillation frequency ensure that there is no consistent bias of the position of the chosen values of b with respect to the phase of the oscillations. In addition, small values of b are weighted less in Eq. (18) than are large values. Therefore this is an accurate integration over the possible values of b.

In order to calculate the final averaged results of the numerical solution to the modified Bloch equations, 1 000 solutions to the differential equations had to be made for each value of the E fields tested. The result averaged over b and t_0 for the case of Na-Ar collisions is presented in Fig. 11. The number density of Na (target) atoms was set to 10^{14} cm^{-3} and the number of Ar (perturber) atoms was set to 2×10^{18} cm^{-3}. Runs were done for both 1.6-psec pulses (short) and 10-psec pulses (long). At low intensities the number density excited is calculated to be greater for the 10-psec pulse than for the 1.6-psec pulse. This is because at the same electric field strength the 10-psec has six times more photons than does the 1.6-psec pulse. In order to compare properly the excitation probability for these two curves the results were divided by the pulse width to take out this bias. The result, shown in Fig. 12, is proportional to an excitation efficiency per incident laser photon, and is also proportional to the collision quasi-cross-section defined in Eq. (21). As predicted, the short pulse does have a higher excitation efficiency or collision cross section than a long pulse at high intensities, although the ratio is not as great as that predicted by Lee and George[5] and illustrated in Fig. 4. The reason for this is that even at the highest E fields where the excitation probability is reduced in the long-pulse case, there are two points in time during the Gaussian temporal pulse shape where the E field is indeed equal to $E_{\rm crit}$. Therefore the population in this case is generated not at the peak of the long pulse but rather by collisions which occur on the temporal wings of the pulse where the E field happens to be $E_{\rm crit}$.

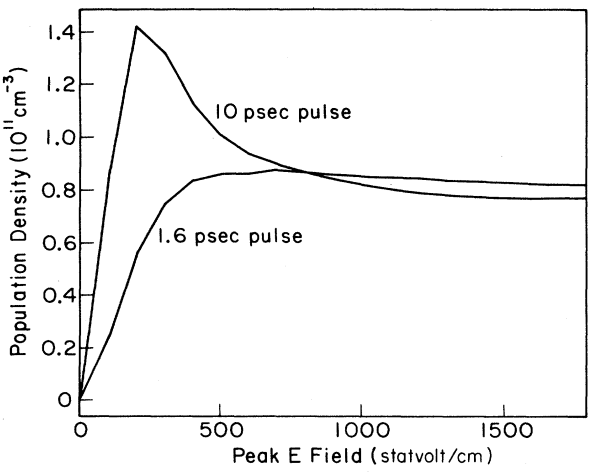

FIG. 11. E-field dependence of excitation number density for short and long pulses when averaged over both impact parameter (b) and time delay (t_0). Sodium density is 10^{14} cm^{-3} and argon density is 2×18^{18} cm^{-3}. Parameters are same as in Fig. 6.

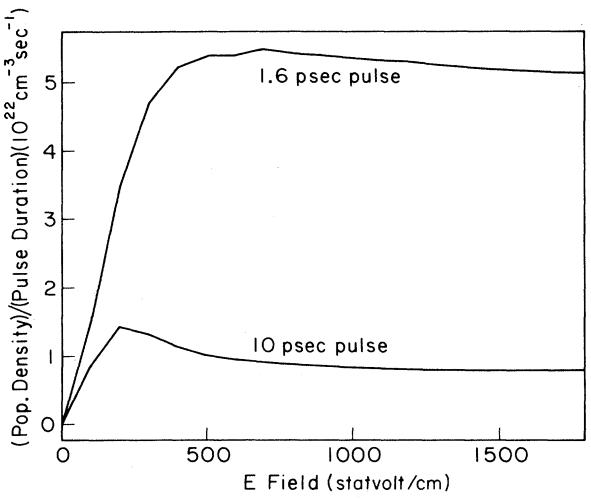

FIG. 12. Results of Fig. 11 divided by the pulse duration to take out the bias of increased photon number with longer pulses. The result is proportional to an excitation efficiency per laser photon, or to a collision quasi-cross-section.

6. *Average over laser-beam profile*

Experimentally it is difficult to generate a laser pulse whose spatial profile is square, or uniform across the diameter of the beam, without introducing large energy losses. Therefore, in practice one generally uses a beam with a spatially varying intensity. In experiments such as those described in this work this does have a large effect since the desired result is strongly intensity dependent.

In order to model this effect the results of the excitation-probability calculation Eq. (18) are integrated over the interaction volume to find the total number N_T of excited-state atoms produced,

$$N_T(E_0,\tau_p,\Delta_L) = \int\int\int N_{\rm ex}(E(x,y,z),\tau_p,\Delta_L)\,dx\,dy\,dz\ . \quad (22)$$

With the laser-field distribution given by $E(x,y,z) = E_0\exp[-(x^2+y^2)/2\sigma^2]$, the total number becomes

$$N_T(E_0,\tau_p,\Delta_L) = \frac{2\pi L}{\sigma^2}\int_0^{E_0} N_{\rm ex}(E,\tau_p\Delta_L)\frac{dE}{E}\ , \quad (23)$$

where L is the length of the interaction volume along the z axis.

This calculation was made for the case of Na-Ar collisions excited by a laser pulse with a spatial width parameter $\sigma=50$ μm. The results are plotted in Fig. 13. Since experimentalists measure intensity rather than E

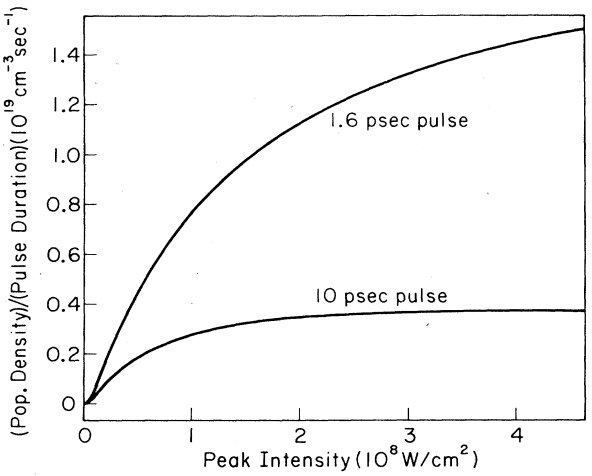

FIG. 13. Spatially averaged result for Na-Ar collision. The horizontal axis is plotted in peak intensity rather than electric field strength in order to make it more comparable with the experimental results. After fully averaging the numerical solution, the difference between the long and short laser pulses is not quite as dramatic.

field, the horizontal axis is in units of W/cm^2. As one can see, the difference between the two cases of long and short pulses is further decreased by the effects of spatial averaging.

7. *Theoretical conclusions*

Calculations based on the theory using Bloch equations produce results similar to those of the simple Landau-Zener model and the extended Landau-Zener model of Lee and George.[5] Averaging over realistic values of both the temporal and spatial beam parameters, however, has a dramatic effect on the results. This is to be expected since a beam of varying intensity is being used to probe highly nonlinear effect. The results still predict, however, that the effect should be seen if the experiment is done with sufficient signal-to-noise ratio.

Assumptions made in developing this theory are reasonable, barring one—the assumption of a two-state target atom. As discussed in Sec. II B 1, Light and Szöke indicated the need to include potential curves arising from all degenerate substates when observing the variation in excitation efficiency with E field. The dramatic difference at high E field was shown to be diminished when three degenerate states were accounted for. Coupled with the effects of both temporal and spatial averaging which also tend to reduce the difference (see Fig. 13) this could make the distinction between short and long pulses difficult to observe.

III. EXPERIMENTAL STUDY

The system studied experimentally is Na-Ar collisions excited by short laser pulses detuned about 15 Å to the long-wavelength side of the Na D_1 line at 5896 Å. Optical collisions induced population in the $3P_{1/2}$ level of Na, which then emitted D_1-line photons, which were detected.

A. Experimental apparatus

1. *Laser system*

The laser system has been described elsewhere.[26–28] Briefly, a frequency-doubled cw modelocked Nd:YAG laser (where YAG represents yttrium aluminum garnet) is used to synchronously pump a rhodamine 6G dye laser. Addition of a second jet of 3,3′-diethyloxadicarbocyanine iodide (DODCI) (which acts as a slight saturable absorber) cleans the pulse temporally and eliminates any satellite pulses. Through the use of various combinations of Lyot filters and étalons the pulsewidth at a wavelength of 5910 Å can be varied from 800 fsec to greater than 50 psec. Part of the unconverted 1.064 μm light is used to seed a cw pumped regenerative amplifier operating at a repetition rate of 1 kHz. Since the output of the regenerative amplifier is synchronized in time to the cw modelocked Nd:YAG laser, and thereby to the dye laser, one of the weak dye-laser pulses can by synchronously amplified by using the output of the regenerative amplifier to pump a three-stage dye amplifier chain. The resulting output pulse has a pulsewidth equal to that of the input pulse, and an energy up to 10 μJ at a repetition rate of up to 1.5 kHz. The ratio of amplified spontaneous emission to laser pulse energy after the dye amplifier is excellent, with a figure greater than 5000 to 1.

2. *Na-Ar vapor cell*

The Na-Ar cell used was a heat pipe operating in oven mode. A 1-in.-diameter stainless-steel cross was used with plate glass windows sealed with Viton O rings on all four ports. Inside the cell, a nickel wick was placed at the center, extending 10 cm into all four ports. The middle of the cell was heated using nichrome wire wrapped around a ceramic wire mold. The ends of each of the ports were cooled by flowing water through copper tubing soldered to the sides. In practice, sodium metal was placed into the center of the cross and heated in a high pressure of Ar. The argon used was a high-purity research grade and was maintained at 250 Torr for most experiments. For the experiments reported in this work the temperature of the cell was maintained at about 300 °C, as measured on the outside of the cell. Equivalent width measurements made of the vapor pressure inside the cell indicated, however, that the temperature inside the cell was nearly 75 °C cooler.

3. *Detection system*

The experimental arrangement used to measure the optical collision fluorescence signal at 5896 Å is shown in Fig. 14. The laser pulse passes through a set of crossed polarizers with a half-wave plate between them. Rotation of the wave plate varies the amount of pulse energy transmitted by the second polarizer and therefore

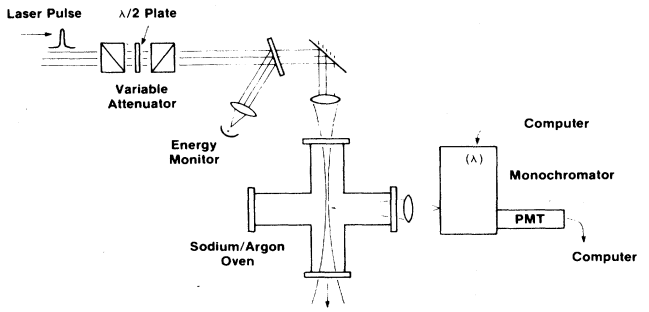

FIG. 14. Experimental configuration used to measure the dependence of the fluorescence intensity on laser intensity and detuning and argon density.

focused into the cell. The second polarizer is oriented such that transmitted light is vertically polarized. The transmitted pulse energy is monitored by using a 4% beam splitter to send part of the beam to a calibrated photodiode. The output of the photodiode is sent to a computer so that for each laser shot the energy can be recorded. The laser beam is then focused into the center of the vapor cell using various lenses. Different lenses are used to adjust the spot size at focus, and thereby the input-laser intensity, in the interaction region. Spot sizes were accurately determined by raster scanning a 3-μm pinhole at the beam focus. The beam is estimated to be no more than 10% greater than diffraction limited. Knowledge of the pulse duration, the spot diameter, and the pulse energy all combine to allow an accurate recording of the laser-input intensity for each shot.

The fluorescence is imaged onto the slit of a 0.3-m spectrometer used in conjunction with a high-speed, high-gain photomultiplier tube (EMI9816B) to measure the fluorescence intensity. The output of the photomultiplier tube is gated and integrated for a 100-nsec period, and the resulting voltage is sent to an analog-to-digital converter which is interfaced to a computer, with the amount of charge generated being proportional to the amount of scattered light at the given wavelength. The gated detection discriminates against certain competing signals which have long decay times, such as ionization followed by recombination.

In order to measure the intensity dependence of the detected signals the spectrometer was set to look only at the peak value of the D_1,D_2 fluorescence components or the Rayleigh-scattering component. Since the spectrometer resolution is large, the peak value is proportional to the area under the component. A large two-dimensional histogram was then created in the computer's memory. For each laser shot 1 was added to the bin which represented the measured fluorescence intensity (for the spectral line of interest) at the measured laser pulse energy. 150 000 shots were taken (2.5 minutes at the 1-kHz repetition rate) for each run, allowing good statistics to be obtained. After each run the number of shots and the average fluorescence intensity were calculated for each laser energy by examining the two-dimensional histogram. The number of shots was then used with a threshold value to accept only those results that had enough laser shots to generate the required statistical significance. Generally 500 shots per laser energy bin were required. In order to test whether this technique introduced any nonlinear dependence, the intensity of laser light scattered from the sides of the cell was measured over the full range of the histogram and was found to be linear with input laser intensity, as it should be.

B. Effects of radiation trapping

When resonance radiation is emitted in the middle of an optically thick vapor, there is a large probability that the radiation will be reabsorbed and reemitted before it escapes from the vapor cell. This effect, radiation trapping, can lead to a loss of signal, depolarization of the emitted light, and an increase in the decay time of the observed fluorescence.

Due to reabsorption of the fluorescence photons, the effective decay rate Γ_{eff} decreases as[29]

$$\Gamma_{\text{eff}}=g A_{21} , \tag{24}$$

where A_{21} is the Einstein coefficient and g is the average probability that a photon emitted from the center of the cell will escape without reabsorption. The value g is termed the "escape factor" and depends on the optical depth at line center, the geometry of the cell, and the type of broadening mechanisms present.[20,30–33] For our particular cell geometry, there are no successful theoretical models that simply describe the effects of radiation trapping.

ac Stark shifting of atomic lines has been used in the past to overcome the effects of radiation trapping.[34] When the laser pulse used to excite the atoms has a pulse duration which is longer than the decay time of the atoms, then the atoms fluoresce at the ac-Stark-shifted wavelengths. Atoms which are outside the laser beam are not Stark shifted and therefore do not absorb the Stark-shifted fluorescence. In our case, however, the laser pulse duration is much shorter than the natural decay time of the Na atoms and therefore the amount of ac-Stark-shifted fluorescence is negligible.

Experimentally there are three radiation trapping effects which occur and which must be noted when interpreting the experimental data. The first is the loss of signal. When light is emitted from the center of the cell it must traverse a 10-cm region of unexcited Na atoms. As it passes down this tube it can be absorbed by a ground-state Na atom, which later fluoresces in a random direction. This randomizing of the direction of propagation decreases the amount of signal collected in two ways. First, there is fluorescence that is trapped and reradiated in a direction such that it hits the wall of the cell and is lost. Second, as the light is reradiated it propagates in a different direction and thus is not imaged onto the slit of the spectrometer by the collection optics.

The second effect which must be noted is the increase in the decay time of the emitted fluorescence. The time delay which occurs as the photons are absorbed and

reemitted causes the observed decay time to increase by the factor $1/g$. Monte Carlo techniques[35] have been used to describe this increase for small values of $1/g$ (<10) and have indicated that the time dependence becomes nonexpotential for values of $1/g$ greater than 3. These effects have been observed experimentally.[33,35]

The third effect involves the scrambling of the emitted polarization by reabsorption of the emitted fluorescence. The reemitted photons can have a random polarization orientation compared to the absorbed photons because of collisions between absorption and emission. Studies of the polarization of the emitted fluorescence must be carried out in an experimental arrangement which does not include the effects of radiation trapping.[10]

Simple estimates of whether or not radiation trapping will be a factor can be made by calculating the peak absorption coefficient of the resonance line and then calculating the Beer's absorption depth for different atomic densities. For the experimental conditions present in these experiments an absorption depth of ten Beer's lengths for the emitted fluorescence photons is calculated. This indicates that radiation trapping will affect our fluorescence data. At a Na density of 2×10^{12} cm^{-3} we observed that the lifetime of the D_1 fluorescence increased to 41 nsec from its natural time of 16 nsec.

In the present experiments, where only the laser-intensity dependence of the fluorescence is examined, the effects of radiation trapping do not alter the dependence— rather they only alter the amount of signal obtained. In this case a high perturber number density can be used in order to increase the observed signal.

C. Absence of amplified-spontaneous-emission-induced excitation and nonadiabatic excitation

Amplified spontaneous emission (ASE) generated in the dye amplifiers can be a serious problem when performing off-resonance studies. Collision-induced fluorescence signals induced by picosecond pulses are extremely weak, and ASE at on-resonance wavelengths can excite the atoms efficiently without the benefit of an optical collision, causing a fluorescence background. Eliminating any ASE is therefore a prime concern. In the dye-amplifier configuration used, a saturable absorber is employed between the first and second stages to absorb any ASE generated in the first stage. Proper adjustment of the absorber dye jet at focus is critical to ensure that the ASE is completely removed. There is little ASE generated in the second stage (since a mild focus is used there) and what is generated is not very directional. Two pinholes are used to aperture the beam and spatially clean any ASE away.

These two methods have eliminated any effects of ASE in the experiments. In order to demonstrate this, three experiments were performed. First, the laser input to the amplifier was blocked so that only ASE is generated. All Na fluorescence signal then disappeared, indicating that all the signal generated was entirely due to the ultrashort laser pulse. Second, a variation of the argon buffer-gas pressure should only change the collisionally redistributed signal and not any direct line excitation. Figure 15 shows the D_1 fluorescence versus Ar pressure for a 1.6-psec pulse with three different peak intensities.

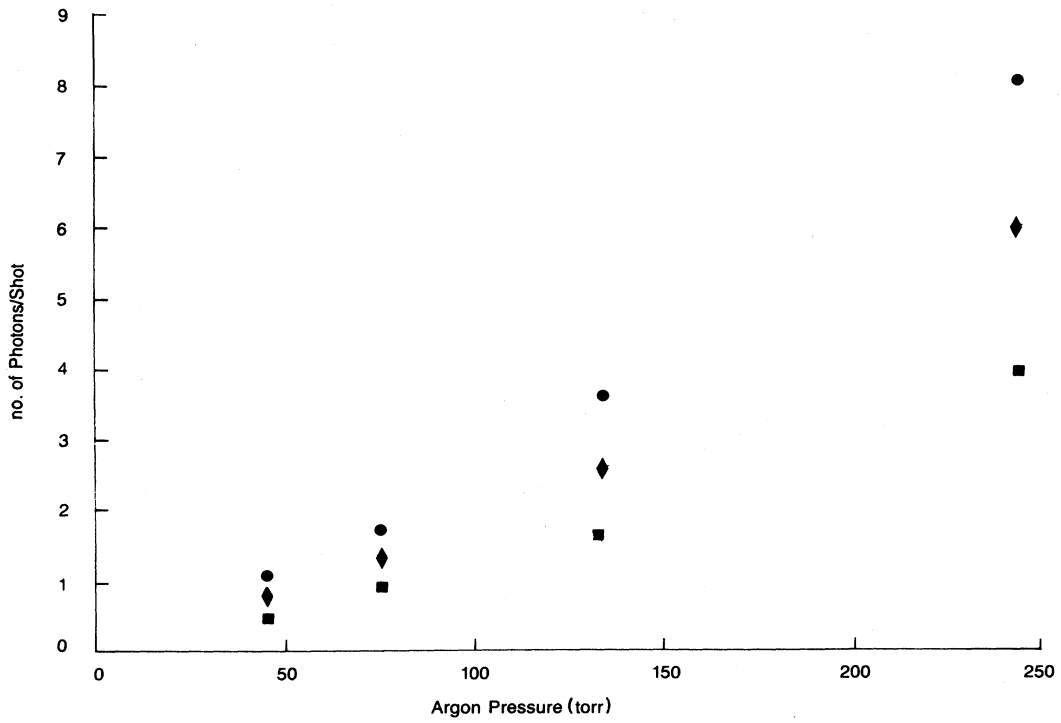

FIG. 15. Fluorescence intensity of the D_1 line vs argon pressure for a 1.6-psec laser pulse and Na density of 8×10^{12} cm^{-3}. Three laser intensities are shown. Squares, 1×10^{11} W/cm^2; diamonds, 2×10^{11} W/cm^2; circles, 3×10^{11} W/cm^2.

The strong dependence of fluorescence on Ar pressure indicates the fluorescence is collision induced. The deviations from the expected linear dependence could be due to radiative trapping; at higher Ar pressure the Na D_1 line has less absorption at line center, causing less trapping and thus larger collected signal. Third, the variation with laser detuning was measured for a 1.6-psec pulse. Direct line excitation due to ASE would not cause rapid decrease in signal with increased detuning; however, this rapid decrease was observed as shown in Fig. 16.

The slope of the solid lines in Fig. 16 is determined from line-shape data.[19] The data at the largest detunings does not fit this slope, which could be due to the fact that at higher detunings the time between curve crossings gets shorter and thus a 1.6-psec pulse moves from being a short pulse to being a long pulse as the detuning is increased. According to Fig. 12 this would give a larger excitation efficiency at higher detunings.

As a further check on the consistency of the measurements, the absolute detected fluorescence signal was compared with the predictal signal. The collection efficiency from photons emitted to photoelectrons detected was measured to be 5×10^{-5}. (See Ref. 36 for details.) The collection volume was 1×10^{-4} cm^3. At a Na density of 2×10^{11} cm^{-3} radiative trapping effects should be small. At this Na density, and an Ar density of 2×10^{18} cm^{-3}, we detected 0.02 photoelectrons per shot from a 1.6-psec laser pulse with peak intensity 1×10^8 W/cm^2. This number of photoelectrons corresponds to 400 excited Na atoms emitting photons. This can be compared to the theoretical results in Fig. 13, which, when corrected for atomic densities, predicts 2 000 excited Na atoms in the collection volume. This reasonable agreement between observed and predicted signals supports our identification of the observed signal as being due to collisional redistribution. Given all of these results, ASE causing excitation without the benefit of a collision seems to have been ruled out as an experimental difficulty.

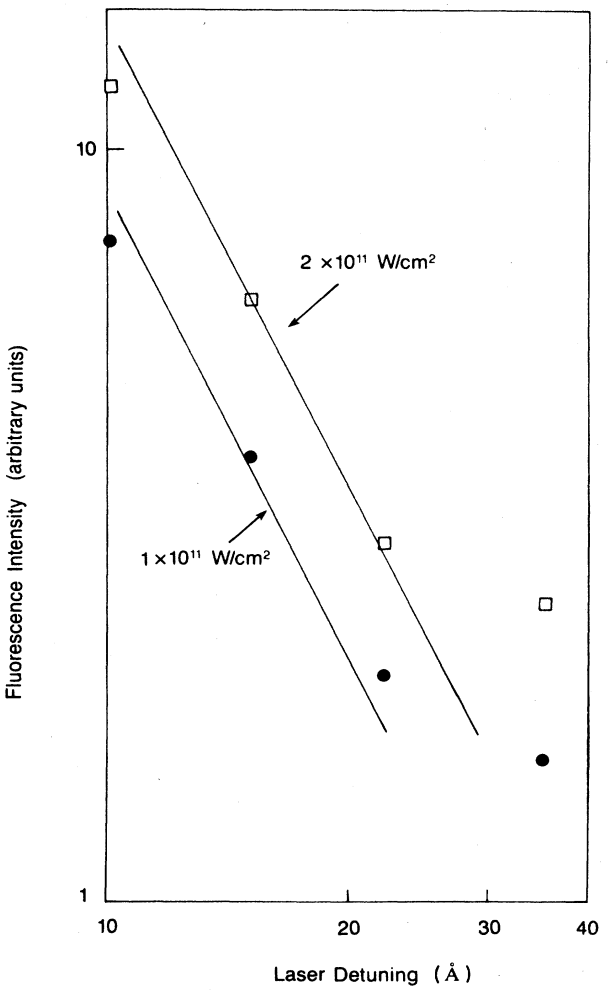

FIG. 16. Fluorescence intensity of D_1 line vs laser detuning, plotted on a log-log scale for two peak laser intensities. The slope (−1.5) of the solid lines is from line-shape data (Ref. 19).

As discussed in Sec. II B 2, even an ideal Gaussian-shaped laser pulse can cause on the order of 1% nonadiabatic excitation of Na atoms not undergoing collisions. The experiments discussed in the previous paragraphs indicate that this degree of nonadiabatic excitation, which would be comparable to that induced by collisions, is *not* taking place. The most likely explanation for this result is that before the laser pulse reaches the detection volume, it passes through 10 cm of Na vapor, corresponding to about 20 Beer's lengths on resonance. This would absorb out all resonant frequency components of the laser pulse, thereby preventing direct excitation. Since the fractional energy absorbed out of the pulse is small, no easily noticeable pulse distortion would be expected. A small-amplitude oscillation at the detuning frequency should be superposed on the pulse envelope.

D. Confirmation of stable picosecond pulse propagation

As demonstrated by Nakatsuka and Grischkowsky,[37] when a near-resonant picosecond pulse propagates through an absorbing medium it can be reshaped and distorted due to the group velocity dispersion and attenuation caused by the vapor. We experimentally examined this effect for the cell and vapor pressures used for our experiments by recording intensity autocorrelation traces before and after the cell. It was found to have no measureable effect on the shape of the 1.6-psec pulse. This is primarily due to the fact that our atomic-number density is 1000 times less than that of Nakatsuka and Grischkowsky.

E. Fluorescence versus laser intensity

Using the experimental technique detailed in Sec. III A 3 the collision-induced fluorescence intensity versus input intensity was measured for different laser-pulse durations. For short pulses with peak intensity between 10^6 and 10^9 W/cm^2 the fluorescence signal was found to be linear in laser intensity. This is in contrast to the theoretical prediction that saturation should start to be

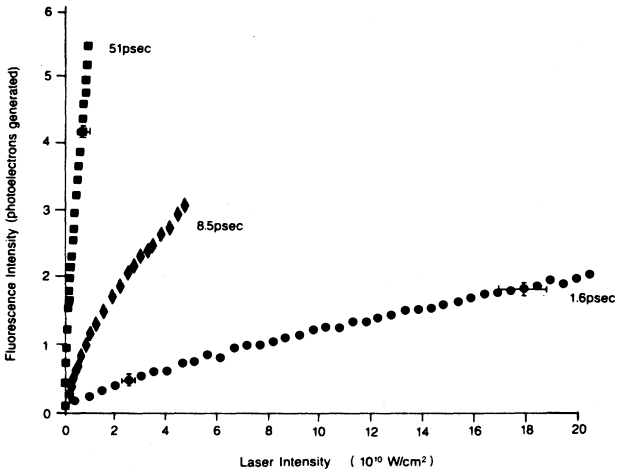

FIG. 17. Fluorescence intensity of the D_1 line vs input laser intensity for three values of the pulse duration. Sodium density was 4×10^{12} cm^{-3} and argon density was 4×10^{18} cm^{-3}.

observed at about 10^7 W/cm^2. At intensities above 10^9 W/cm^2 the results shown in Fig. 17 were obtained. In this case the laser detuning was 15 Å (43 cm^{-1}), the sodium number density was 4×10^{12} cm^{-3} and the argon number density was 4×10^{18} cm^{-3}. As predicted by the theory the fluorescence signal at a given intensity value is much higher for longer pulses than for short pulses due to the difference in the number of photons present in the two laser pulses. For this reason the fluorescence signal was divided by the corresponding pulse duration and the results below 1×10^{10} W/cm^2 are plotted in Fig. 18. This result demonstrates the difference in excitation efficiency for short pulses versus long pulses. In the Na-Ar case the time between curve crossings is about 2.3 psec, so a 1.6-psec pulse is a short pulse whereas the 8.5-psec and 51-psec pulses are long pulses. Because a 300-μm slit width was used to collect as much fluorescence as possible, the spatial averaging of the signal over the laser beam profile causes the loss of the dramatic difference between the short and long types of pulses, as previously discussed in Sec. II B 6.

These experiments qualitatively confirm the theoretical prediction that pulses which are short do indeed have a higher excitation efficiency, or quasicollision cross section, than pulses which are long. By comparing Figs. 18 and 13, however, we see that this intensity at which this difference is observable is about 100 times greater than that predicted theoretically.

In all of the experimental runs there appears a slight "turning up" of the expected fluorescence data near the highest values of the laser intensity, which we believe is statistically significant. (See Ref. 36 for more examples.) This can be seen more clearly when the data of Fig. 17 is plotted versus laser energy per pulse, as in Fig. 19. The turning up can be seen to occur on all three curves at a laser input energy of approximately 3 μJ. Since the observed effect seems to be related to input energy and not to input intensity, effects such as self-focusing, multiphoton processes, and off-resonant collision-free excitation apparently cannot account for the observed behavior. The mechanism resulting in the turning up of the data is not understood at this time.

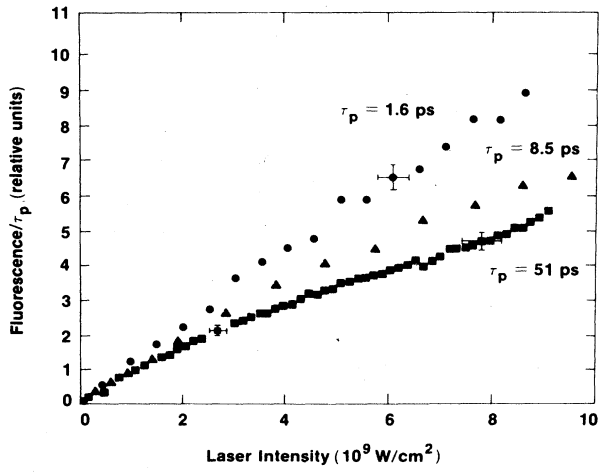

FIG. 18. Fluorescence intensity of the D_1 line (from Fig. 17) divided by the laser pulse duration, vs input laser intensity, for three values of the pulse duration. The fluorescence intensity was divided by the pulsewidth to eliminate the bias caused by the greater number of laser photons in a longer pulse than in a shorter pulse at the same intensity.

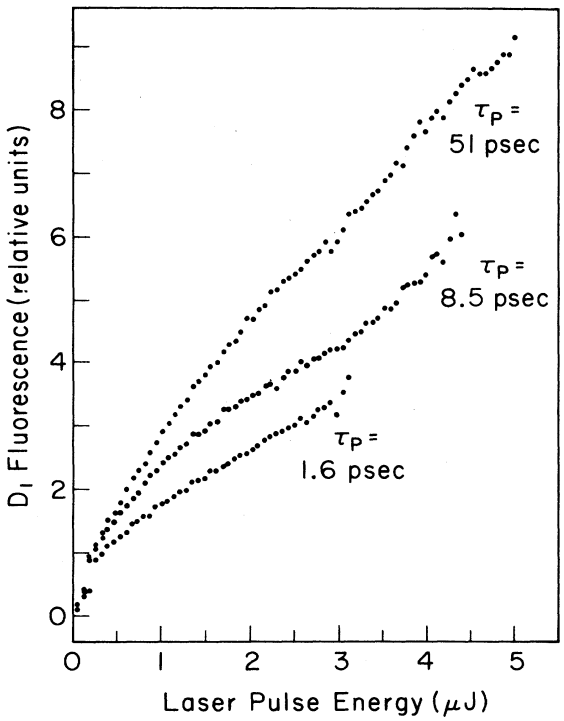

FIG. 19. Fluorescence intensity of the D_1 line (from Fig. 17) vs input laser pulse energy for three different values of the pulse duration.

IV. CONCLUSIONS

A theoretical model has been developed to understand further and predict the interaction of picosecond optical pulses and colliding atoms. This theory includes effects due to realistic laser pulse shapes and beam profiles, which have been shown to have a major impact on the intensity dependence of the collisional redistribution. Following the proposal of Lee and George,[5] a study was carried out of the variation of the collision (quasi-) cross section with laser pulses that are long as well as those that are short in comparison to the time between curve crossings. Lee and George predicted an enhanced collision cross section for short laser pulses, which was theoretically verified by our theory (see Fig. 13), albeit with a reduction in the magnitude of the effect when one uses realistic pulse shapes.

Using a new type of picosecond dye laser system the first experimental study of optical collisions with picosecond pulses has been performed. Despite extremely weak signals, the pulse-width-dependent intensity variation proposed by Lee and George and theoretically confirmed in this work has been experimentally verified (see Fig. 18). Although the cross-section dependence on pulse duration was indeed confirmed, the laser intensity needed was 100 times higher than that theoretically predicted. This is probably due to the effect of multiple excited-state potentials, as first pointed out by Light and Szöke.[4] The excited-state sodium $3P_{1/2}$ and $3P_{3/2}$ levels each correspond to Π molecular states which intersect the laser-dressed ground-state level.[38] Light and Szöke showed for a long pulse that, due to the effect of multiple states, the fall off of the cross section at high laser intensities was not as fast as that predicted by two-state models. Also, with the strong effects of temporal and spatial averaging present, the difference between long and short pulses was further suppressed, requiring much higher electric field strengths to be used.

A more accurate theory than the present one could be developed by including the multiple states in the excited level. A theory of this type of this type was recently developed[38] to explain experiments on the ratio of the D_1 and D_2 line excitations by a cw, low-intensity laser field.[39] The theory would have to be generalized to allow for short, intense laser pulses. Also, more accurate potentials for the Na-Ar system than those used here have been calculated[40] and should be used in an improved theory. Preliminary results of such a theory have been reported.[41]

A theory including all of the relevant potentials would also yield information about the polarization of the fluorescence emitted in the D_1 and D_2 lines. In Sr-Ar experiments with weak cw lasers it was found that polarization measurements give information about the potentials that is not available from total intensity measurements.[42] We conjecture that the fluorescence polarization may depend on laser-pulse duration, especially at high intensities, since excitation of outgoing channels of the collision may depend on pulse duration.

It should be emphasized that the possibility of nonadiabatic excitation by the short pulse, without the occurrence of a collision, complicates the interpretation of the experimental results, as discussed in Sec. III C. Theoretical calculation shows that with a Gaussian-shaped pulse, under our conditions, this effect would be expected to produce an excited-state population comparable to that produced by collisions (although not larger than 2% of atoms, even with peak power as high as 10^{10} W/cm^2). Nevertheless the data shown in Figs. 15 and 16 seem to indicate that the fluorescence observed was due primarily to collisions. A likely resolution to this apparent discrepancy is that the dense Na vapor the laser pulse traverses before reaching the observation region absorbs out those spectral components of the pulse that would most strongly contribute to nonadiabatic excitation. This point should be investigated further.

ACKNOWLEDGMENTS

The authors acknowledge the cooperation of Professor Gerard Mourou, in whose laboratory these experiments were carried out. The high-speed computer code used for data acquisition was developed with the assistance of Lawrence Forsley. This work was supported by National Science Foundation Physics Grant No. PHY-8215132. This work was partially supported by the Laser Fusion Feasibility Project at the Laboratory for Laser Energetics, which has the following sponsors: Empire State Electric Energy Research Corporation, General Electric Company, New York State Energy Research and Development Authority, Northeast Utilities Service Company, Southern California Edison Company, The Standard Oil Company (Ohio), and the University of Rochester.

APPENDIX

Here the procedure of averaging over impact parameter b and time of closest approach t_0, leading to Eq. (18), is developed. Consider the target atom A to be fixed. The number of perturbers within a shell centered on the target atom with radius R and thickness dR is given by $N_P 4\pi R^2 dR$, where N_P is the perturber number density. Given that a perturber P is in this shell, the probability density that it is traveling in a direction (θ,Φ) with respect to the line connecting the atoms is given by $(4\pi)^{-1}\sin\theta$. The spherical coordinate system (R,θ,Φ)

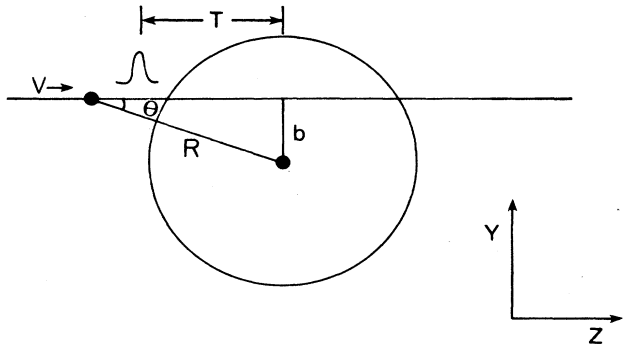

FIG. 20. Perturber P, a distance R from the target atom A, traveling with velocity V in direction θ with respect to the line joining the atoms.

has its origin at the perturber atom P. See Fig. 20. Thus, the number of perturbers at distance $R\pm\frac{1}{2}dR$ traveling in direction $(\theta\pm\frac{1}{2}d\theta,\ \Phi\pm\frac{1}{2}d\Phi)$ is given by $N_P R^2 \sin\theta\, dR\, d\theta\, d\Phi$.

Changing to cylindrical coordinates (b,z,Φ) and integrating over Φ, the number of perturbers with impact parameter $b\pm\frac{1}{2}db$ and distance from closest approach $z\pm\frac{1}{2}dz$ is given by $N_P 2\pi b\, db\, dz$. If the perturber is traveling with velocity V, then $z=Vt_0$ and the number of perturbers with impact parameter $b\pm\frac{1}{2}db$ and time from closest approach $t_0\pm\frac{1}{2}dt_0$ is given by $N_P 2\pi V b\, db\, dt_0$. This, then, provides the weighting factor that is used in Eq. (18).

---

*Also with the Laboratory for Laser Energetics, University of Rochester. Current address: AT&T Bell Laboratories, Holmdel, NJ 07733.

[1]V. S. Lisitsa and S. I. Yakovlenko, Zh. Eksp. Teor. Fiz. **68**, 479 (1975) [Sov. Phys.—JETP **41**, 233 (1975)].

[2]N. M. Kroll and K. M. Watson, Phys. Rev. A **13**, 1018 (1976).

[3]A. M. F. Lau, Phys. Rev. A **13**, 139 (1976).

[4]J. C. Light and A. Szöke, Phys. Rev. A **18**, 1363 (1978).

[5]H. W. Lee and T. F. George, J. Phys. Chem. **83**, 928 (1979).

[6]S. Yeh and P. R. Berman, Phys. Rev. A **19**, 1106 (1979).

[7]P. D. Kleiber, J. Cooper, K. Burnett, C. V. Kunasz, and M. G. Raymer, Phys. Rev. A **27**, 291 (1983).

[8]W. R. Green, J. Lukasik, J. R. Willison, M. D. Wright, J. F. Young, and S. E. Harris, Phys. Rev. Lett. **42**, 970 (1979).

[9]A. M. Bonch-Bruevich, T. A. Vartanyan, and V. V. Khromov, Zh. Eksp. Teor. Fiz. **78**, 538 (1980) [Sov. Phys.—JETP **51**, 271 (1980)].

[10]P. D. Kleiber, K. Burnett, and J. Cooper, Phys. Rev. Lett. **47**, 1595 (1981).

[11]J. Lukasik and S. C. Wallace, Phys. Rev. Lett. **47**, 240 (1981).

[12]P. Pillet, R. Kachru, N. H. Tran, W. W. Smith, and T. F. Gallagher, Phys. Rev. Lett. **50**, 1763 (1983).

[13]A. Omont, E. W. Smith, and J. Cooper, Astrophys. J. **175**, 185 (1972); **182**, 283 (1973).

[14]J. L. Carlsten, A. Szöke, and M. G. Raymer, Phys. Rev. A **15**, 1029 (1977).

[15]See, however, A. Szöke, Opt. Lett. **2**, 36 (1978).

[16]See also P. D. Kleiber, Ph. D. thesis, University of Colorado (1982); and K. Burnett, Phys. Rep. **118**, 339 (1985).

[17]T. Sizer II and M. G. Raymer, Phys. Rev. Lett. **56**, 123 (1986).

[18]R. E. M. Hedges, D. L. Drummond, and A. Gallagher, Phys. Rev. A **6**, 1519 (1972).

[19]W. R. Hindmarsh, A. D. Petford, and G. Smith, Proc. R. Soc. London, Ser. A **297**, 296 (1967).

[20]J. Huennekens and A. Gallagher, Phys. Rev. A **28**, 238 (1983).

[21]V. L. Landau, Z. Phys. Sov. **2**, 46 (1932).

[22]C. Zener, Proc. R. Soc. London, Ser. A **137**, 696 (1932).

[23]E. C. G. Stueckelberg, Helv. Phys. Acta **5**, 369 (1932).

[24]D. R. Bates, Proc. R. Soc. London, Ser. A **257**, 22 (1960).

[25]See, for example, L. Allen and J. H. Eberly, *Optical Resonance and Two Level Atoms* (Wiley, New York, 1975).

[26]T. Sizer II, J. D. Kafka, I. N. Duling III, C. W. Gabel, and G. A. Mourou, IEEE J. Quantum Electron. **QE-19**, 506 (1983).

[27]T. Norris, T. Sizer II, and G. Mourou, J. Opt. Soc. Am. B **2**, 613 (1985).

[28]I. N. Duling III, T. Norris, T. Sizer II, P. Bado, and G. A. Mourou, J. Opt. Soc. Am. B **2**, 616 (1985).

[29]T. Holstein, Phys. Rev. **72**, 1212 (1947).

[30]T. Holstein, Phys. Rev. **83**, 1159 (1951).

[31]C. van Tright, Phys. Rev. **181**, 97 (1969); Phys. Rev. A **13**, 726 (1976).

[32]M. G. Payne, J. E. Talmage, G. S. Hurst, and E. B. Wagner, Phys. Rev. A **9**, 1050 (1974).

[33]J. B. Anderson, J. Maya, M. W. Grossman, R. Lagushenko, and J. F. Waymouth, Phys. Rev. A **31**, 2968 (1983).

[34]P. Wiorkowski and W. Hartmann, Opt. Comm. **53**, 217 (1985).

[35]M. Braun, H. Liening, B. Storr, and P. Wiorkowski, Opt. Comm. **53**, 217 (1985).

[36]T. Sizer II, Ph. D. thesis, University of Rochester (1985).

[37]H. Nakatsuda and D. Grischkowsky, Opt. Lett. **6**, 13 (1981).

[38]K. C. Kulander and F. Rebentrost, J. Chem. Phys. **80**, 5623 (1984).

[39]M. D. Havey, G. E. Copeland, and W. J. Wang, Phys. Rev. Lett. **50**, 1767 (1985).

[40]R. Düren, E. Hasselbrink, and G. Moritz, Z. Phys. Abt. A **307**, 1 (1982); R. P. Saxon, R. E. Olson, and B. Liu, J. Chem. Phys. **67**, 2692 (1977).

[41]P. De Vries, Bull. Am. Phys. Soc. **31**, 927 (1986).

[42]W. J. Alford, K. Burnett, and J. Cooper, Phys. Rev. A **27**, 1310 (1983).